



# NOF1 encodes an arabidopsis protein involved in the control of rRNA expression

Erwana Harscoet, Bertrand Dubreucq, Jean-Christophe Palauqui, Loic Lepiniec

## ► To cite this version:

Erwana Harscoet, Bertrand Dubreucq, Jean-Christophe Palauqui, Loic Lepiniec. NOF1 encodes an arabidopsis protein involved in the control of rRNA expression. PLoS ONE, 2010, 5 (9), pp.e12829. 10.1371/journal.pone.0012829 . hal-01203890

**HAL Id: hal-01203890**

**<https://hal.science/hal-01203890>**

Submitted on 30 May 2020

**HAL** is a multi-disciplinary open access archive for the deposit and dissemination of scientific research documents, whether they are published or not. The documents may come from teaching and research institutions in France or abroad, or from public or private research centers.

L'archive ouverte pluridisciplinaire **HAL**, est destinée au dépôt et à la diffusion de documents scientifiques de niveau recherche, publiés ou non, émanant des établissements d'enseignement et de recherche français ou étrangers, des laboratoires publics ou privés.

# NOF1 Encodes an Arabidopsis Protein Involved in the Control of rRNA Expression

Erwana Harscoët, Bertrand Dubreucq, Jean-Christophe Palauqui, Loïc Lepiniec\*

INRA, UPB, UMR 1318 INRA-AgroParisTech, Versailles, France

## Abstract

The control of ribosomal RNA biogenesis is essential for the regulation of protein synthesis in eukaryotic cells. Here, we report the characterization of *NOF1* that encodes a putative nucleolar protein involved in the control of rRNA expression in Arabidopsis. The gene has been isolated by T-DNA tagging and its function verified by the characterization of a second allele and genetic complementation of the mutants. The *nof1* mutants are affected in female gametogenesis and embryo development. This result is consistent with the detection of *NOF1* mRNA in all tissues throughout plant life's cycle, and preferentially in differentiating cells. Interestingly, the closely related proteins from zebra fish and yeast are also necessary for cell division and differentiation. We showed that the *nof1-1* mutant displays higher rRNA expression and hypomethylation of rRNA promoter. Taken together, the results presented here demonstrated that *NOF1* is an Arabidopsis gene involved in the control of rRNA expression, and suggested that it encodes a putative nucleolar protein, the function of which may be conserved in eukaryotes.

**Citation:** Harscoët E, Dubreucq B, Palauqui J-C, Lepiniec L (2010) *NOF1* Encodes an Arabidopsis Protein Involved in the Control of rRNA Expression. PLoS ONE 5(9): e12829. doi:10.1371/journal.pone.0012829

**Editor:** Markus Grebe, Umeå Plant Science Centre, Sweden

**Received:** February 15, 2010; **Accepted:** August 13, 2010; **Published:** September 20, 2010

**Copyright:** © 2010 Harscoët et al. This is an open-access article distributed under the terms of the Creative Commons Attribution License, which permits unrestricted use, distribution, and reproduction in any medium, provided the original author and source are credited.

**Funding:** This work was supported by the French Genoplante Program. The funders had no role in study design, data collection and analysis, decision to publish, or preparation of the manuscript.

**Competing Interests:** The authors have declared that no competing interests exist.

\* E-mail: lepiniec@versailles.inra.fr

## Introduction

In order to identify genes involved in seed development or cellular housekeeping functions, several laboratories have used the model plant Arabidopsis for performing large-scale genetic screens [1,2]. From these studies, the number of non-redundant genes essential for cell growth, division, and differentiation during gametophytes or/and seed development was estimated above 500 [3,4]. Some of these genes have been shown to encode for proteins that are involved in nucleolar functions [5,6,7,8,9,10,11]. The nucleolus is known to be involved in biogenesis of ribosome-subunits in eukaryotic cells [12,13]. The initial ribosomal RNA (rRNA) precursor transcript is cleaved to form the mature 28S, 18S, and 5.8S rRNAs that are post-transcriptionally modified, through interactions with small nucleolar ribonucleoproteins (snoRNPs) [13,14]. Then, with the help of other processing factors, rRNAs are assembled and exported into the cytoplasm. In Human, proteomic approaches have led to the identification of around 700 nucleolar proteins [15]. In plants, more than 200 nucleolar proteins have been identified [15,16,17]. A comparison of the nucleolar proteome from humans and yeast showed that 90% of human proteins have yeast homologues, thus demonstrating the strong conservation of nucleolar proteome through evolution [15]. However, plant and human nucleoli display some significant differences [16,17,18] and only 70% of the plant nucleolar proteins identified have human homologues (<http://bioinf.scri.sari.ac.uk/cgi-bin/atnodb/home>).

Here, we report the isolation and functional characterization of *NOF1* that encodes for a nucleolar protein showing strong similarities with two proteins of yeast (YIL091C, accession n° Y21428) and zebra fish (DEF, accession n° Q6PEH4) [19]. The

three conserved proteins appear to be necessary for the control of cell division or differentiation. Interestingly, the yeast protein interacts with several nucleolar proteins involved in rRNA biogenesis. In agreement with this function, we showed that the *nof1* mutants are affected in the methylation of rDNA promoter and rRNA expression.

## Results

### Isolation of the two allelic mutants *nof1-1* and *nof1-2* that are affected in embryo development

A visual screening for abnormal seed morphologies of the Versailles' collection of T-DNA insertion lines was performed allowing the isolation of about 250 mutants [4]. One of these mutants, named *nucleolar factor 1-1* (*nof1-1*), was obtained in the progenies of the "DKE14" primary transformant. Plants hemizygous for the mutation appeared normal, except for the production of some wrinkled brown seeds (Figure 1a–c). Cytological analyses showed that the mutant seeds contain abnormal embryos, the development of which is arrested from early in the phase of pattern formation, to late in the maturation phase [20] (Figures 1g–k and S1). Although some of the developed *nof1-1* embryos were still metabolically active (Figure S1-B), the mutant seeds were unable to germinate. Consistent with this observation, the segregation analyses suggested that *nof1-1* mutation was recessive, monogenic, and lethal (Table S1). No homozygote plants for the mutation have been obtained. In addition, a strict co-segregation of the T-DNA (providing kanamycin resistance) with the abnormal wrinkled-seed phenotype was observed in the progenies of 110 plants. These results suggested the presence of a single T-DNA

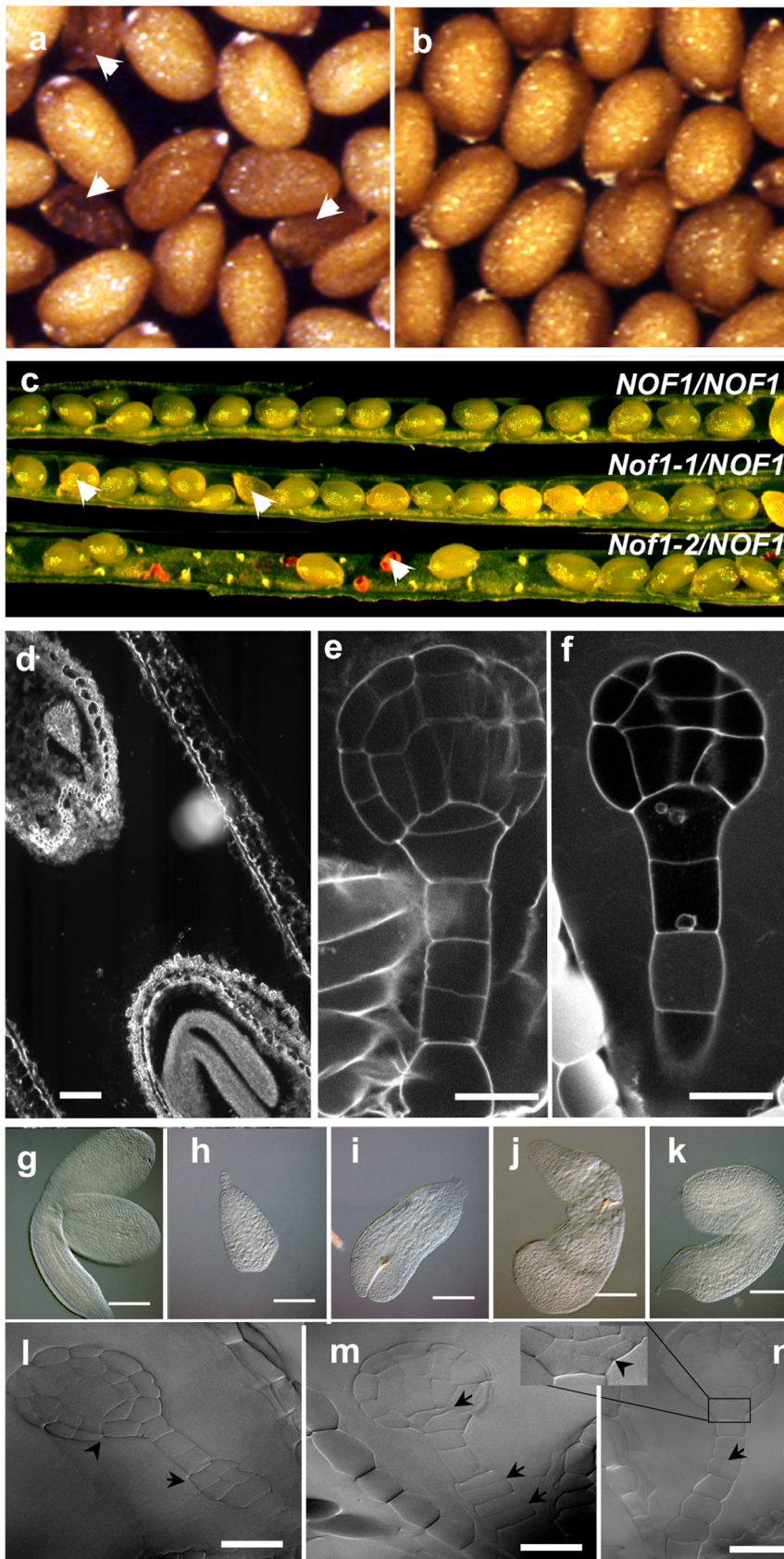


**Figure 1. Phenotypic analyses of wild type and *nof1-1* mutant seeds.** (a) Mature dry seeds from *nof1-1/NOF1-1* hemizygous plants displaying a few dark brown mutant seeds (indicated with arrows) and (b) Wild-type (Ws) control seeds. (c) representative developing siliques of wild-type accession (Ws) that displays immature green seeds (top row); *nof1-1/NOF1-1* (weak allele) genotype that display white (i.e. lethal) seeds (second row); and *nof1-2/NOF1-2* genotype (third row) that display gaps (i.e. missing seed) and shrunken empty seed coat for the null allele *nof1-2*. (d) Late developmental stage in a single silique comparing a *nof1-1* mutant embryo (top left) to a wild type embryo (bottom right). Laser scanning confocal image of Ws embryo (e) compared to *nof1-1* globular embryo with abnormal cell divisions (f). Wild type embryo extracted from mature seed (g) compared to several *nof1-1* embryos arrested at different stages of development (h–k). DIC images of *nof1-1* embryos with abnormal cell divisions (arrows). Bars = 600  $\mu$ M (a, b, c), 10  $\mu$ M (e, f, l, m, n), 100  $\mu$ M (g–k). doi:10.1371/journal.pone.0012829.g001

insertion locus in *nof1-1*, which was genetically linked to the mutation. Supporting this conclusion, DNA hybridization experiments with T-DNA specific probes showed that a single T-DNA was present in the mutant (data not shown). After the molecular identification of the *NOF1* gene, a second T-DNA insertion mutant named *nof1-2* was identified by reverse genetics screening in the progenies of the EXY42 primary transformant. No genetic complementation was observed when crossing two hemizygous lines (*NOF1/nof1-1* with *NOF1/nof1-2*), confirming that both mutants were allelic. Consistent with the embryo lethal phenotype of *nof1-1*, no homozygous plants were obtained with the *nof1-2* mutation.

### Gametes transmission is affected in the *nof1* mutants

Segregation analyses showed that the number of seedlings resistant to kanamycin was significantly lower than expected for a dominant marker linked to a lethal mutation (63% for *nof1-1/NOF1*  $n=2361$  and 29% for *nof1-2/NOF1*  $n=915$ , instead of 66.66%. Table S1). These segregations suggested that the mutated alleles, and more especially *nof1-2*, were transmitted to the progeny at a lower frequency than the wild-type allele. These results were consistent with the molecular analyses demonstrating that *nof1-2* is a null allele (see below) with abnormal ovule development (Figure 1c). Cytological analysis of cleared ovules showed that the putative *nof1-2* ovules were arrested during the mitotic divisions of the megagametogenesis (Figure S2). The reciprocal crosses between wild-type and hemizygous mutants lines confirmed that the transmission of *nof1-2* alleles was null through the female gametes and reduced through pollen (Table S2).

### The *nof1-1* mutant is affected in cellular division pattern

In the wild-type developing embryo cells divide following a precise pattern [2]. Cytological observations revealed irregular pattern and/or additional cell divisions in *nof1-1* embryos (Figures 1d–f and S3A and B). The number of cell layers was sometime locally increased. In addition, lack of cell adhesion was found in embryos that are bent at the middle of the hypocotyl (Figure S3B). Although present, both meristems exhibited abnormalities such as a flat apical meristem or abnormal quiescent

center in the root (Figure S3B). Taken together these data suggested that *nof1-1* embryos are affected in orientation and number of cell divisions. In addition, *NOF1* was preferentially expressed in differentiating cells (see hereafter and Figure 5A). In order to test if these phenotypes were associated with auxin signaling, the expressions of *pDR5:GUS* marker [21] and the localization of the auxin transporter PIN1 [22] were monitored in the mutant background. The reporter construct *pDR5:GUS* was introduced by crossing into *nof1-1* background and the localization of PIN1 was carried out by immunolocalization. In both cases, no striking differences were observed between the developed *nof1-1* and wild type embryos (Figure 2). Therefore, the abnormal *nof1-1* cellular phenotypes were probably not due to a default in auxin signaling. Nevertheless, they give an explanation to the abnormal development of *nof1-1* embryos.

### Isolation and molecular characterization of *NOF1*

Isolation of the putative *NOF1* gene was performed using the T-DNA tagged *nof1-1* allele. Plant genomic sequences flanking the left (68 bp) and right (73 bp) T-DNA borders were recovered by walking PCR and sequenced [23]. The site of integration was assigned to chromosome 1 in the intergenic region at 195 bp upstream the ATG initiation codon of At1g17690 (Figure 3A). A small deletion of 33 bp was found at the insertion locus. A second allele was isolated by reverse genetic using FlagDB [24]. Localization of the T-DNA insertion (7 kb) in the gene suggested that *nof1-2* is likely a null allele (Figure 3A). In order to confirm the identity of *NOF1*, the genetic complementation of both alleles was obtained with a wild-type genomic clone (see material and methods and Figure S4). Taken together these data showed that *NOF1* is At1g17690. This gene encodes a putative protein of 754 amino-acid residues of unknown function. Sequencing of a cDNA and complementation of the *nof1-1* mutant with this cDNA fused to GFP confirmed this prediction (see next paragraph). The protein contains a potential nucleolar localization signal (NoLS) [25] and a conserved “DUF1253” domain of unknown function (Figure 3A). Only one *NOF1* gene is found in Arabidopsis and closely related genes were found in other eukaryotes (Figure 3B). For instance, DEF from danio [19] and YIL091C from yeast

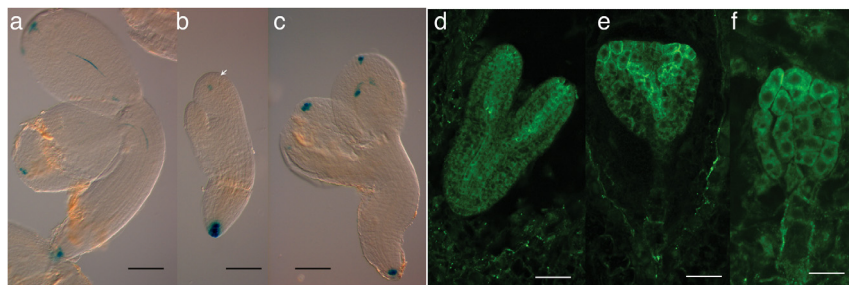


**Figure 2. Auxin signaling in *nof1-1*.** PRO<sub>DR5</sub>: uidA expression in wild type (a) and mutants (b and c) embryos. Immunolocalization of PIN1 in wild type (d) and *nof1-1* mutants (e and f) embryos. Bar = 40  $\mu$ M (a to c) and 100  $\mu$ M (d to f). doi:10.1371/journal.pone.0012829.g002



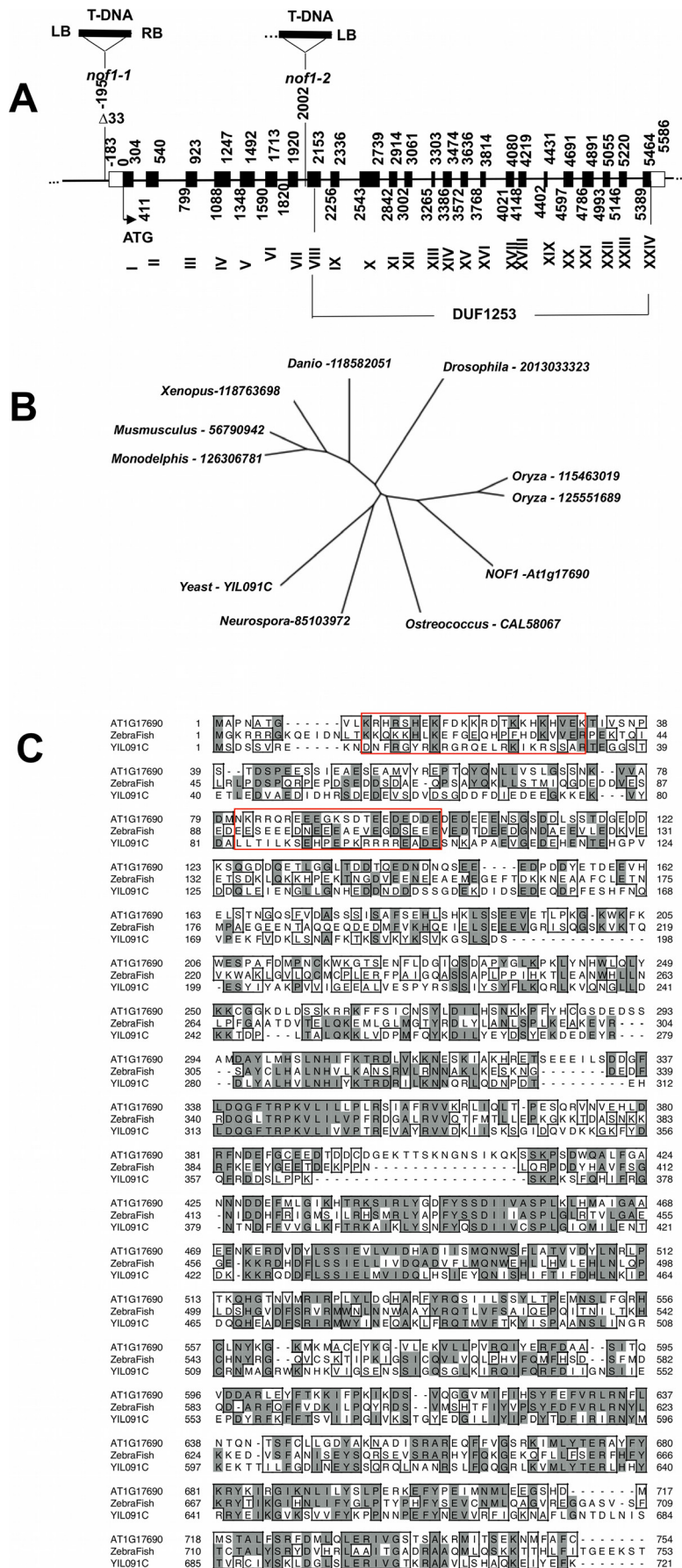


**Figure 3. Molecular characterization of *NOF1*.** **A)** Schematic representation of the structure of the *NOF1* (At1g17690) locus in wild type and *nof1-1* and *nof1-2* mutants. The structure of the gene is deduced from the comparison between genomic and cDNA sequences. In *nof1-1*, the T-DNA was inserted between positions –195 to –228 relative to the ATG (first codon), leading to a small deletion of 33 bp. In *nof1-2*, a T-DNA is inserted after nucleotide 2002. Boxes are exons. The 5'UTR is predicted according to ESTs sequences. Location of the DUF1253 domain is indicated below the scheme. **B)** Unrooted neighbour-Joining tree representing the distance between NOF1 and the most closely related proteins from various organisms was obtained using the full amino-acid sequences, after clustal W alignment (<http://align.genome.jp/>). **C)** Deduced amino acid sequences of NOF1 and closely related proteins are presented (At1g17690: NOF1, Zebrafish (DEF): gj37046654, and yeast YIL091C). Identities between amino acid residues are shown with dark boxes and similarities with light boxes. The putative NoLS site is boxed.  
doi:10.1371/journal.pone.0012829.g003

display about 50% identities at the amino-acid level (Figure 3C). This may indicated a conserved function among eukaryotes.

### *NOF1* is expressed in all tissues, but preferentially in differentiating cells

The expression of *NOF1* was investigated in various tissues by RT-PCR. *NOF1* mRNA was detected in all organs tested (Figure 4A). These results were fully consistent with transcriptomic data available (Figure S5). Interestingly, in the weak mutant allele (*nof1-1*), some *NOF1* mRNA was still detected at 2 days after pollination (Figure 4B), probably due to the insertion of the T-DNA in the promoter region. This result was consistent with the weak phenotype of *nof1-1* compared to that of the null *nof1-2* (the latter does not produce embryos). However, it is difficult to fully avoid the hypothesis of a contamination by mRNA from the carpel. The spatio-temporal activity of the *pNOF1* promoter was then investigated in transgenic plant that express the *pNOF1::GUS* reporter construct. GUS activity was mainly detected in cells that undergo cellular differentiation in young tissues such as floral buds, ovules, embryo, secondary roots, pollen, young seedlings and vascular bundles (Figure 5A).

### *NOF1* is a nucleolar protein

In order to investigate intracellular localization of NOF1, a *NOF1::GFP* chimeric gene was introduced in a *nof1-1* hemizygous plant. Primary transformants exhibiting complementation of the *nof1-1* phenotype in their progenies were obtained, indicating that the chimeric construct was functional. By comparison with DAPI staining of the nucleus, a nucleolar localization of GFP was observed in young developing ovules (Figure 5B). No GFP was detected in other tissues suggesting a weak stability of the chimeric protein. The *NOF1::GFP* chimeric gene was transiently expressed in tobacco cells giving a similar result, with a preferential accumulation in the nucleolus (Figure 5B).

It is known that modifications of nucleolar functions can affect the size of the nucleolus [10]. Therefore, a cytological analysis of the nucleus was made. Although no obvious differences were observed earlier in nucleolus morphology, the *nof1-1* cells showed enlarged nucleoli at the globular and heart stages of embryo

development (Figure 6A). Image analyses, at the globular stage of embryo development, confirmed that although the size of the nuclei is not affected in *nof1-1* (Figure 6B), the nucleoli are significantly enlarged (Figure 6C). These data argue in favor of an important role for NOF1 in the nucleolus.

### The accumulation of rRNA increases in *nof1-1*

The yeast structural ortholog of NOF1 (i.e. YIL091C) has been recently shown to interact with nucleolar proteins MPP10 and SAS10 [26]. MPP10 and SAS10 are members of the small subunit of the rRNA processome (SSU) [27,28,29,30]. These data are fully consistent with the nucleolar localization of NOF1 and the abnormal phenotype of the nucleoli in *nof1-1* cells. Furthermore in silico analysis of genes co-expressed with *NOF1* revealed a strong bias for ribosome function as compared with randomly generated lists of genes (Figure S6).

Processing of the pre-rRNA is conserved among eukaryotes and has been described in details [5,12,14,31,32,33]. The pre-rRNA is firstly cleaved at the P site located in the 5' external transcript spacer (ETS) and then in the internal transcript spacers (ITS) (Figure 7). To confirm the involvement of NOF1 in rRNA biogenesis, the levels of pre-rRNA and mature 18S, 5.8S, and 25S rRNAs were monitored by quantitative RT-PCR (Figure 7). RNAs were extracted from mutant embryos obtained from white seeds collected in developing siliques at 2 and 11 days after pollination. In *nof1-1*, a strong increase in pre-rRNA accumulation was observed (Figure 7A). Similar increases were found for total rRNAs (Figure 7B). These results showed that the *nof1-1* mutation triggered a strong increase in rRNA expression.

### The methylation of rRNA promoter is affected in *nof1-1*

In plants, rDNA transcription is regulated by methylation of the promoter region [34,35]. In Arabidopsis, the transcription start site (TSS) of the Polymerase I was shown to be methylation sensitive and to contain specific elements of regulation [36]. Interestingly, it has been recently shown that YIL091C, the putative yeast homolog of NOF1, interacts with JHD2, an histone (H3K4) demethylase [37,38]. The methylation of histone 3 lysine 4 is an epigenetic mark

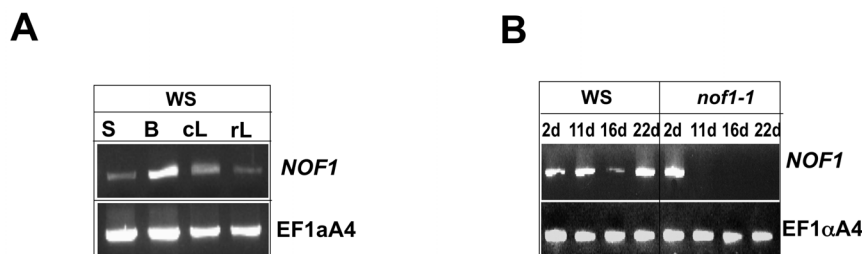


**Figure 4. Analyses of *NOF1* mRNA accumulation in wild type and *nof1-1*.** RNA was extracted from various plant organs (**A**) and seeds (**B**) at different stages of development and used for reverse transcription. Primers specific for *NOF1* and for *EF1aA4* as control were used on the same set of first strand cDNA templates generated with dT primers. During silique development (**B**), WS or *nof1-1* seeds were manually dissected based on seed phenotype to produce the *NOF1* cDNA template at 2, 11, 16 and 22 days after fertilization. S: seeds, B: buds, cL: cauline leaves, rL: rosette leaves.  
doi:10.1371/journal.pone.0012829.g004

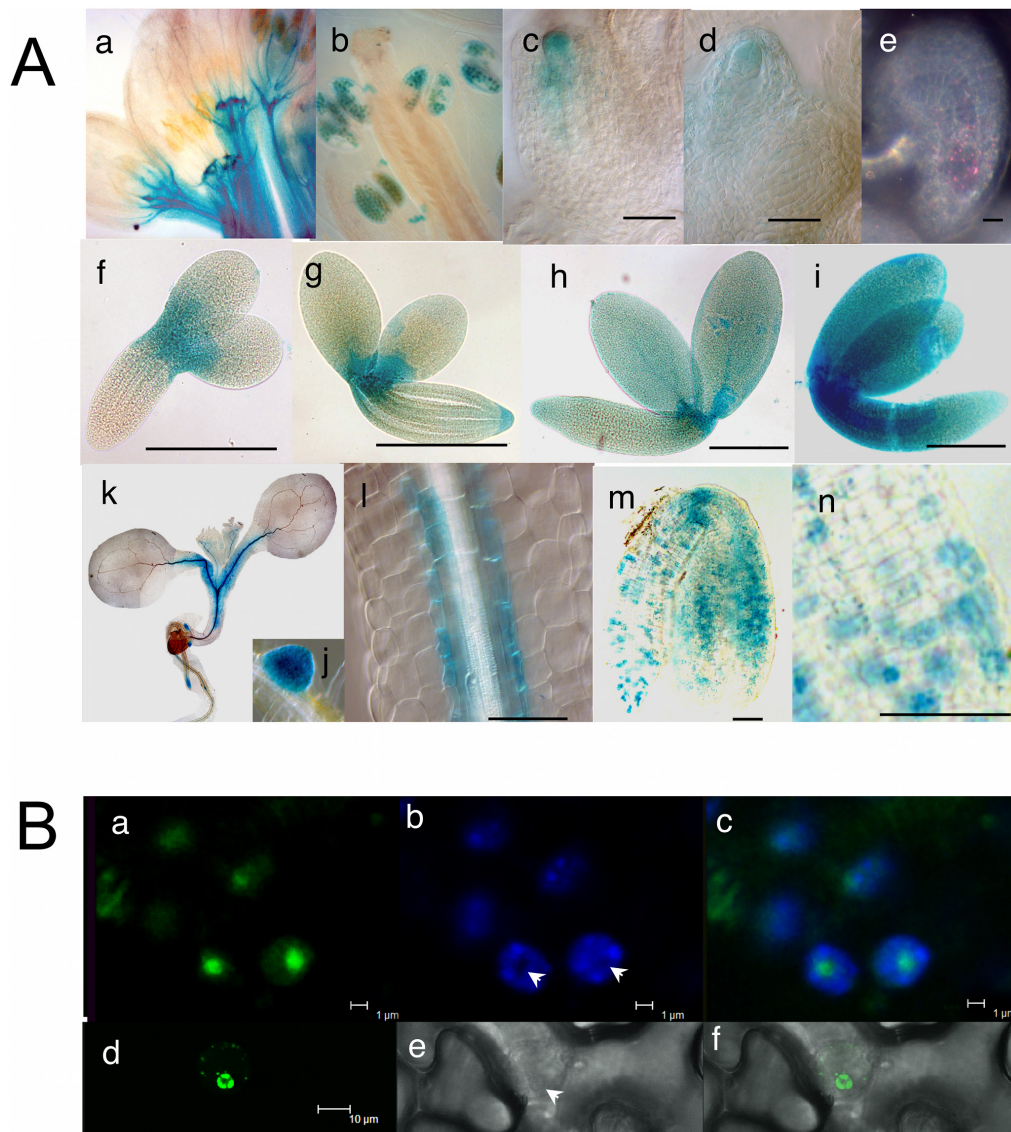


**Figure 5. Cytological analyses of *NOF1* expression and intracellular localization of the protein.** **A** The activity of the *NOF1* promoter (*pNOF:Uida*) was investigated in various plant organs. The result of GUS activity was observed with Nomarski optics, except for (e) where dark field is used, on flowers (a–b) showing expression in buds and in pollen. Expression was found in the nucellus of developing ovules (c–d) and later in the embryo sac (e). During embryogenesis, GUS activity is found at the top of the hypocotyl and extends throughout the embryo during maturation (f to i). After 24 h of imbibition, the expression is found with a patchy pattern in the embryo (l to n) before disappearing. Five days after imbibition's start, the expression is found in root apex (k), lateral root initials (j) and around vascular bundles (l). Bars = 10  $\mu$ m (c to e), 100  $\mu$ m (f to i) and 50  $\mu$ m (l to n). **B**. Subcellular localization of *NOF1:GFP* in transgenic Arabidopsis lines expressing *35S:NOF1:GFP*. GFP is detected in the nucleoli (a), DAPI staining (b) and merged image (c). Transient expression in tobacco leaves of *35S:NOF1:GFP* showing nucleolar localization of *NOF1:GFP* (d), transmitted light (e), and merged pictures (f). Bar = 1  $\mu$ m (a, b, c) and 10  $\mu$ m (d, e, f). doi:10.1371/journal.pone.0012829.g005

that triggers DNA hypomethylation and thus increases transcription [39]. Therefore, it is tempting to speculate that the strong expression of rRNA in *nof1-1* could be due to the hypomethylation of rDNA promoter. To test this hypothesis, the level of methylation of rDNA promoter was investigated by quantitative RT-PCR after restriction of genomic DNA with a methylation sensitive enzyme (*HpaII*). Amplifications were performed with TSS specific primers on DNA templates extracted from *nof1-1* dissected seeds, at 11 days after pollination (Figure 8). This method was more suitable than conventional bisulfite conversion for the limited amount of biological materials available after seed dissection and produced reproducible results [40,41]. The rDNA promoters were signifi-

cantly less methylated in *nof1-1* than in hemizygous embryos (Figure 8). In addition, the methylation of 25S rDNA region used as control was not affected in *nof1-1*. These results suggested that rDNA promoter is specifically hypomethylated in *nof1-1* that is consistent with higher expression of rRNA.

## Discussion

### *NOF1* is required for embryogenesis and gametogenesis in Arabidopsis

In this study, we have shown that *NOF1* is essential for female gametogenesis and embryogenesis. The leaky allele *nof1-1*, that

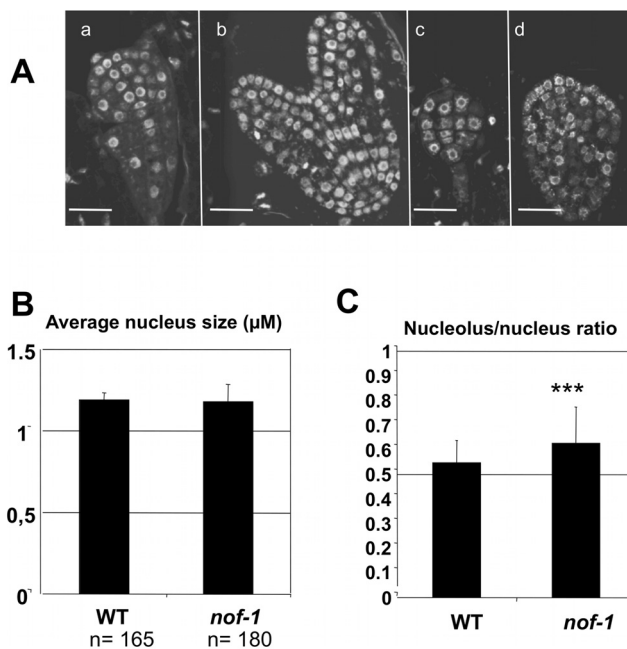


**Figure 6. Nucleolus phenotypes.** **A)** Embryo development at the globular and heart stage of development, Ws (a and b respectively) and *nof1-1* (c and d respectively) after DAPI staining and laser confocal imaging. Bar = 5 μm. **B)** Average nucleus diameter was measured in Ws and *nof1-1* embryos after DAPI staining and laser scanning confocal imaging. **C)** Average ratio of nucleolus vs nucleus diameters in Ws compared to *nof1-1*. A student test was performed to compare both populations of nucleoli, demonstrating a significant difference with  $p < 0.0001$  ( $t = -6.26$ ).  
doi:10.1371/journal.pone.0012829.g006

accumulates *NOF1* mRNA until a few days after fertilization, produced embryos exhibiting a broad range of abnormal cellular phenotypes (e.g. cell division pattern or lack of cell adhesion). These data are consistent with the expression data demonstrating that *NOF1* is expressed in all tissues, and preferentially in dividing cells. Since auxin is an important hormone in embryo development [42,43,44,45,46], we have investigated whether it may be involved in these abnormal cellular phenotypes. The immunolocalization of the PIN1 auxin transporter as well as the use of Pro<sub>DR5</sub>:GUS construct in the *nof1-1* mutant background did not reveal any obvious changes in auxin transport and accumulation. These results indicated that the abnormal cellular phenotypes are very likely not the consequence of a modified auxin accumulation or transport. The strongest *nof1* allele is impaired very early during female gametogenesis and the male gametogenesis is slightly affected. This result is fully consistent with the finding that several proteins involved in general cell cycle progression, including nucleolar proteins such as *SLOW WALKER 1* (*SWA1*, At2g47990) [5], play essential roles during female gametogenesis. Nevertheless, we cannot rule out the possibility that a redundant function may exist in pollen. In addition, although *NOF1* mRNA was found in all tissues, we do not know if *NOF1* is really necessary for cell viability in all tissues during the entire plant life cycle. To answer these questions it would be interesting to build an inducible dominant negative system (e.g. RNAi) to switch off *NOF1* expression in specific tissues and cells.

### NOF1 is involved in nucleolar functions

Sequence analysis of the predicted *NOF1* protein revealed potential nucleolus localization signal (NoLS) [47] in the N terminal part of the

protein. In addition, the yeast ortholog (i.e. YIL091C) has been recently shown to interact with several nucleolar proteins [26]. The functional data reported here, both in tobacco and in Arabidopsis are consistent with a nucleolar localization of *NOF1*. Interestingly, despite the complementation of *nof1-1* abnormal phenotype by the ectopic expression of *NOF1:GFP* construct, GFP signal was detected only in the integuments of developing ovules. This result suggested a post-translational control of *NOF1* in vegetative parts. A putative sumoylation site on lysine (K205) was also predicted using SUMOsp program [48]. Sumoylation is a reversible post-translational modification that appears to play a crucial role in a variety of biological processes [49]. It would be interesting to investigate if the putative sumoylation site is involved in *NOF1* functions.

Consistent with the putative nucleolar localization of *NOF1*, its mutation affects the size of the nucleoli. A similar increase was previously reported in other embryo lethal mutants [8,10]. In both cases, the mutated gene were directly linked to nucleolar functions and ribosome biogenesis. On this line, a link between rDNA transcription and the size of the nucleolus was recently reported using inhibitors of DNA methyl transferases [50]. Taken together these data showed that *NOF1* encodes a putative nucleolar protein, the function of which is important for the nucleolus, in agreement with its involvement in rRNA biogenesis.

### NOF1 is involved in the control of rRNA expression

In *nof1-1*, an increase in rRNA expression was observed, in association with hypomethylation of the rDNA promoter region. These genetic analyses support the view that *NOF1* acts through rDNA transcription and is fully consistent with the demonstration that rDNA methylation negatively impacts rDNA transcription by polymerase I [34,35,36,51,52,53,54]. As *NOF1*, the closely related yeast (YIL091C) and danio (DEF) proteins are localized in the nucleus and are essential for cell viability [19,55] suggesting a functional conservation of these proteins. Furthermore, DEF was shown to affect cellular differentiation and division as *def* mutants exhibit an arrest of expansion growth of digestive organs [19]. Interestingly, in yeast, YIL091C interacts with a H3K4 demethylase [37,38] and demethylation of H3K4 leads to DNA methylation and inhibition of rDNA transcription [56]. On the same line, JHDM1B, a human nucleolar demethylase of the same family (i.e. containing a JmjC domain), controls the repression of rDNA gene expression by specific demethylation of trimethylated H3K4, limiting cell growth and proliferation [57]. Therefore, a similar mechanism likely occurs in plants supporting the view that *NOF1* is involved in a network of proteins acting through a chromatin-based regulation of rDNA transcription. In order to confirm this molecular role, it would be necessary to set up an inducible system *in planta* (e.g. RNAi) allowing to test the direct effect of switching off *NOF1* expression on H3K4 methylation and to search for JmjC demethylase homolog in Arabidopsis. Interestingly, a related JmjC-domain gene has been recently characterized, the mutation of which triggers ectopic cytosine methylation, probably through an increase in H3K9 methylation levels [58]. Last, it is worth to notice that the loss of JHD2 demethylase in yeast is not lethal, suggesting that the mutation of YIL091C would affect other nucleolar functions, in agreement with its interactions with several nucleolar proteins.

### A putative network of proteins involved in nucleolar functions

Among the proteins interacting with YIL091C are SAS10 and MPP10 [26], both involved in rRNA biogenesis. SAS10 plays a role in the structure of silenced chromatin [29], likely through H3 and H4 acetylation [59]. MPP10 is a part of the small subunit



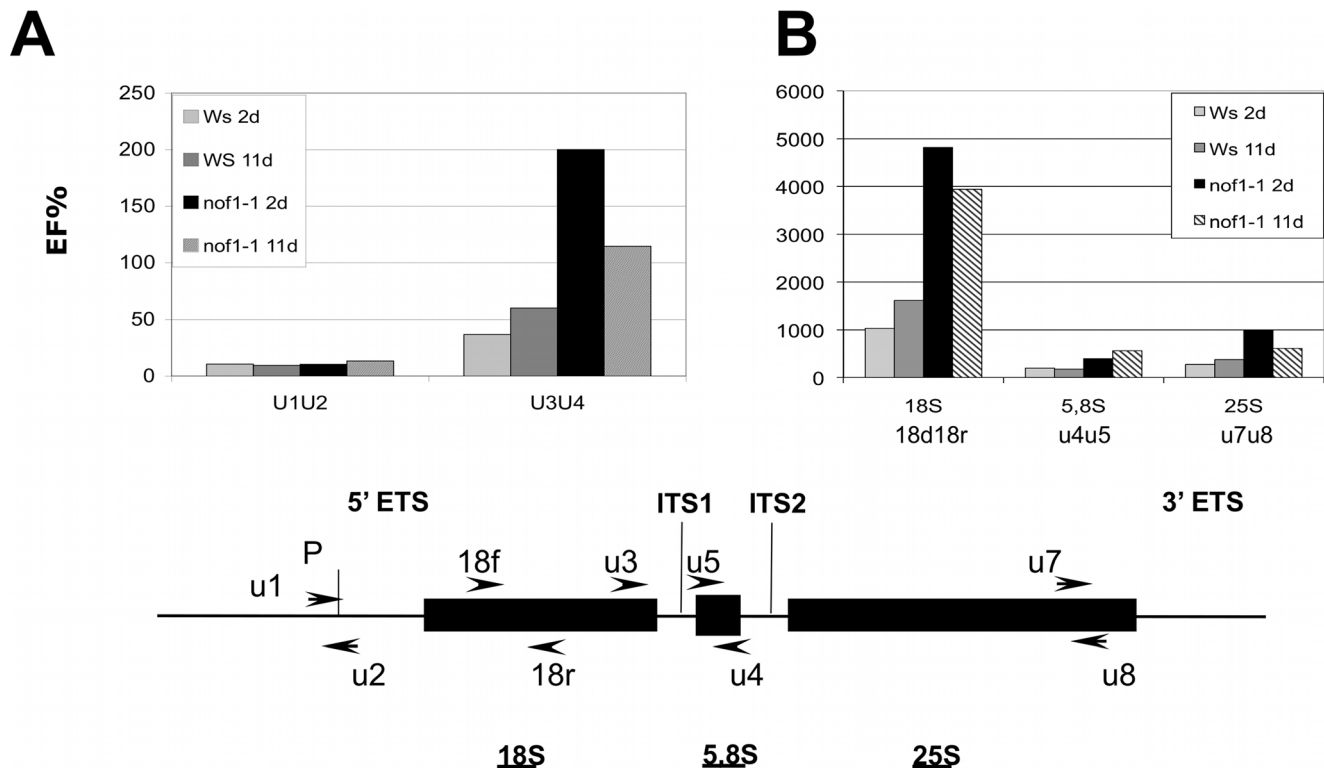


**Figure 7. Expression and processing of the 45S rRNA.** Accumulation of rRNA was monitored by qRT-PCR using specific primers for unprocessed (U1/U2, U3/U4) (A) and processed forms (i.e. 18S f/r, U5/U4 for 5.8S and U7/U8 for 25S) (B) of the 45S rRNA transcript. The cDNA templates were obtained after manual seeds dissection from a hemizygous plants for the *nof1-1* mutation or wild-type (Ws), at 2 or 11 days after fertilization. One representative experiment of three independent biological repeat is shown.  
doi:10.1371/journal.pone.0012829.g007

processome (SSU) required for rRNA biogenesis [14,27,28,60]. Comparative genomics between *Arabidopsis* and yeast [61,62] revealed a putative network of homologous proteins that could interact with NOF1 to control rRNA biogenesis (Figure S7). The genetic and functional characterizations of some of these proteins strongly support this hypothesis. For instance, SWA1 is a nucleolar protein, expressed in dividing cells, essential for female gametogenesis and involved in rRNA biogenesis [5]. TORMOZ (TOZ, At5g16750) is a nucleolar protein, required for cell division patterning, at least during embryo development (no null allele have been characterized), that may be also involved in rRNA biogenesis [7]. Therefore, it is tempting to speculate that a similar network of nucleolar proteins, including NOF1, is involved in the regulation of rRNA biogenesis in *Arabidopsis*. As in yeast, NOF1 and interacting proteins would constitute a molecular link between the regulation of rDNA gene expression and processing of rRNA, by filling the gap between the processome and the transcription of rDNA. Nevertheless, although coupling of rRNA biogenesis with cell growth has been established [12,63,64,65], we cannot exclude that other nucleolar functions are affected by *NOF1* mutation (e.g. modification of small RNAs, assembling of ribonucleoproteins, or cell division). For instance, YIL091C was shown to interact with several kinases such as Swe1 that regulates transition from G2/M or Tos3, a tumor suppressor essential to mammalian embryo development [66].

## Materials and Methods

### Plant material, growth conditions and seed viability

*A. thaliana* seeds of the wild-type ecotype Wassilewskija (WS) as well as the primary transformants DKE14 and EXY42 lines were obtained

from the IJPB seed stock center (INRA, Versailles, France, [http://dbsgap.versailles.inra.fr/agrobactplus/English/Accueil\\_eng.jsp](http://dbsgap.versailles.inra.fr/agrobactplus/English/Accueil_eng.jsp)). Seeds were surface sterilized and germinated on Murashige and Skoog (MS) medium (M02 555, pH 5.6; Duchefa, Haarlem, the Netherlands) solidified with 0.7% (w/v) agar. After a cold treatment of 48 h at 4°C in the dark, the plates were transferred to a growth chamber and incubated at 20°C/15°C day/night, under a 16-h/8-h light/dark regime. Selection of T-DNA-containing seeds was performed by germination on MS supplemented with kanamycin (Sigma, Saint-Quentin Fallavier, France) at 50 mg l<sup>-1</sup>. After 15 days, the plantlets were transferred to sterilized compost in individual pots, grown under the same conditions as above and irrigated twice a week with a complete mineral nutrient solution. To analyze the distribution of seeds with phenotype (white and wrinkled seeds), hemizygous *nof1-1/NOF1-1* siliques at 15 DAF were opened and observed without disturbing seed positions. For time course studies, all the developing seeds of one shoot were harvested 3–4 weeks after the onset of flowering; siliques ranging from 3 to 22 DAF were opened and the corresponding seeds removed and subsampled. Material used for RNA extraction was immediately frozen in liquid nitrogen and stored at –80°C prior to extraction.

Viability tests were based on the reduction of tetrazolium salts to highly colored end products called formazans in viable seeds. Teguments of imbibed mutant and wild-type seeds were torn and embryos were soaked in a 1% 2,3,5-triphenyl tetrazolium chloride solution (Sigma, CA). Samples were incubated for 2 days in the dark at 30°C.

### DNA extraction and PCR analysis

RT-PCR experiments were performed as previously described [67]. All the oligonucleotides used in this study are described in

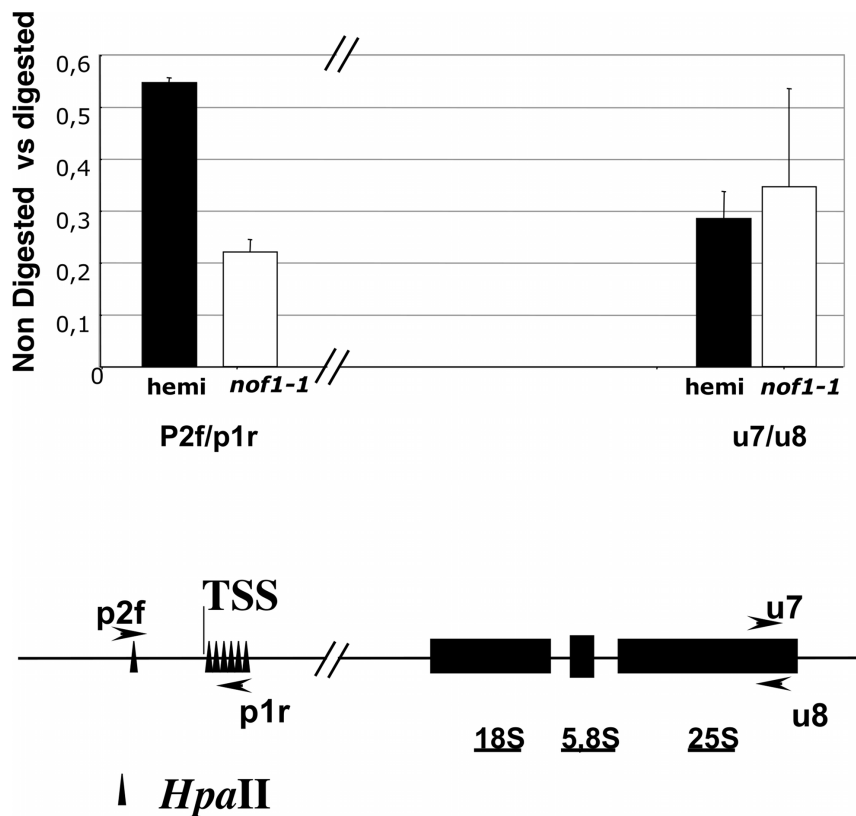


**Figure 8. Quantification of DNA methylation at the 45S rDNA locus.** The level of methylation of the promoter region was estimated by qPCR. Genomic DNA was PCR amplified directly or after restriction with a methylation sensitive enzyme (*HpaII*) using specific primers (p2f and p1r). The amplification of the 25 s rDNA was used as internal control. Results are the means of 3 measurements (+/- standard deviation). Experiments have been made on two independent biological replicates showing similar results. TSS: transcription start site. doi:10.1371/journal.pone.0012829.g008

table S3. Briefly, total RNA was extracted from different tissues using an RNA extraction kit (Mammalian total RNA extraction kit, SIGMA) supplemented with RNase-free Dnase (Qiagen, Germany) during the extraction. cDNAs were synthesized using the Superscript II (INVITROGEN) with (dT)<sub>22</sub> according to the manufacturer's instructions. *NOF1* cDNA was amplified using Stock center cDNA C104805 with the primers B1dke14ATGgate and B1dke14STOPgate located at the start codon and 3'-end of the cDNA, respectively. For gene expression analysis, a 1449 bp fragment of the At1g17690 cDNA was amplified with the primers cDNA dkeUp (5'-GCACAGGTCCCATGAGAAATT-3') and cDNA dkeLow (5'-TGTCAAAGGCAGGTGATTCCCA-3'). Controls were carried out with primers that amplify a constitutively expressed elongation factor 'EF-1alpha' cDNA as previously described [68].

#### Intracellular localization of NOF1

The *NOF1* cDNA was amplified with the proofreading Pfu Ultra DNA polymerase (STRATAGENE, La Jolla, CA, USA) from cDNA obtained after reverse transcription of whole silique-extracted mRNAs using the *B1DKE14ATGgate* and *B2DKE14STP-gate* oligonucleotides. The PCR product was introduced by a BP recombination into *pDONR207* entry vector (INVITROGEN, Carlsbad, CA, USA) and transferred into the binary vector pMDC83 vector [69] by a LR recombination reaction, to obtain a translational fusion between the *NOF1* and the *GFP* (C-terminal) reporter gene. This plasmid was used for stable as well as transient expression of NOF1:GFP.

#### Genetic complementation of the *nof1* mutants

The *NOF1* genomic sequence (7218 bp length, containing 1500 bp of promoter sequence and 500 pb of 3' sequence) was PCR amplified from DNA of the BAC F11A6 and blunt cloned into TOPOblunt vector (Invitrogen Carlsbad, California, USA). A *XhoI/KpnI* fragment was then subcloned into the *KpnI/SalI* restricted pBIB-HYG vector [70]. The resulting plasmid was introduced into *Agrobacterium tumefaciens* strain C58C1 pMP90 [71] by electroporation. Hemizygous plant *NOF1/nof1-1* were transformed by infiltration [72], using surfactant Silwet L-77. Transformants were selected by growing seedlings on hygromycin (50 mg/ml). On the 123 primary transformants obtained, 18 were homozygous for the mutation (*nof1-1*) as suggested by the resistance of their progenies to kanamycin and confirmed by genotyping by PCR (data not shown). The complementation of *nof1-2* allele was obtained by crossing hemizygous plants with complemented homozygous *nof1-1* plants and selecting for homozygous *nof1-2/nof1-2* in their progenies.

#### Functional analysis of the *NOF1* promoter

The *NOF1* promoter used (*Pro<sub>4NOF1</sub>:uid4*) corresponds to region -1500 to -1 bp relative to the translational start codon and was amplified with the proofreading Pfu Ultra DNA polymerase (STRATAGENE, La Jolla, CA, USA) from BACF11A6 using *B1DKE14up* and *B2DKE14low*, *attB1* and *attB2* referring to the corresponding Gateway recombination sequences. The PCR product was introduced by a BP recombination into *pDONR207* entry vector (INVITROGEN, Carlsbad, CA, USA) and trans-

ferred to the binary vector *pBI101-RIR2-GUS* (F. Divol, J.-C. Palauqui, and B. Dubreucq, unpublished data) by a LR recombination reaction, to obtain a transcriptional fusion between the *NOF1* promoter (*pNOF1*) and the *uidA* reporter gene. Arabidopsis transformation was carried out as described above. Ten transformants were selected on MS medium containing kanamycin (50 mg.l<sup>-1</sup>) and then transferred to soil for further characterization.

### Immunolocalization

For immunolocalizations, samples were fixed for 1 h in 4% (w/v) paraformaldehyde embedded, sectioned and treated as previously described [73]. Epitope demasking was carried out by incubating the slides in buffer citrate 10 mM, PH 6 (0.1 M sodium citrate, 0.1 M citric acid) in EZ- RETRIEVER (Biogenex, San Ramon USA). A commercial goat antibody against PIN1 (aP-20, Santa Cruz Biotechnology, ref sc-276163) was used at 1:100. Secondary antibodies were purchased from Molecular Probe (Alexa-conjugated donkey anti goat).

### Imaging and pictures measurements

Light microscopy was carried out as previously described [74]. Briefly, samples were fixed with 4% paraformaldehyde and 5% dimethyl sulfoxide in 0.1 M phosphate buffer pH 7, dehydrated in acetone and included in resin (Technovit 7100 kit, Heraeus Kulzer, Germany), following the manufacturer's instructions. Semi-thin sections (4–8 μm) were performed with a Jung RM 2055 microtome (Leica), stained with toluidin blue (1% w/v in 0.1 M phosphate buffer pH 7.2; Sigma, CA). For analyses using Nomarski optics, seeds were removed from siliques and cleared for 1 to 24 h in a chloralhydrate solution (chloralhydrate-H<sub>2</sub>O-glycerol, 8:2:1, w:v:v) on a microscope glass slide. Samples were examined using an Axioplan II microscope (Zeiss, Jena, Germany) microscope with or without Nomarski optics. Photographs were taken using a progressC10 digital camera (Jenoptik, Jena, Germany). For confocal microscopy, A Leica TCS-SP2-AOBS spectral confocal laser-scanning microscope (Leica Microsystems, Mannheim, Germany) was used. The excitation wavelength for DAPI, GFP and Alexa488 stained samples was 405, 488 nm, respectively emission was collected at 420 to 470 nm and 500–550 nm respectively. Samples for modified pseudo-Schiff propidium iodide staining procedure were prepared and imaged as recently described [75]. Data were processed for 3D volume rendering or 2D orthogonal sections using the open source software Osirix (<http://homepage.mac.com/rossetantoine/osirix/>) on a quadxeon 2,66 Ghz 2 GB RAM Apple Mac pro workstation. RGB stacks of confocal images were imported as DICOM files into Osirix prior to treatments.

### DNA methylation experiments

Genomic DNA was extracted from dissected seeds exhibiting in the same silique either the “white seed” mutant phenotype (*nof1-1*) or wild-type green seeds, using DNA extraction columns (DNeasy plant mini, Qiagen, Courtaboeuf, France). Thus the green seeds are called “hemi” since they contain 2/3 of heterozygous seeds (*nof1-1/NOF1*) and 1/3 of WT seeds. DNA was PCR amplified using specific primers (p2f GCATGCAAAAAGAATTTTCA and p2r CTGGAAAAGGCAACAAAAC) directly or after restriction with a methylation sensitive enzyme (*HpaII* NEB Ipswich USA), following the manufacturer's instructions. The oligonucleotides were designed to amplify a genomic fragment including the transcription start signal and containing 6 *HpaII* restriction sites. The amplification of the 25S rDNA using oligo nucleotides u7 and u8 was used as internal control on both genomic DNA templates

since this fragment does not contain any *HpaII* restriction site. The level of amplification is presented as a percentage of the internal standard *EF1alpha* gene (that contains no *HpaII* site), to normalize genomic DNA variations between samples. Then a ratio between digested versus non-digested genomic DNA samples is calculated. Data presented are representative of 2 independent biological repeats and the error bars show the variations of three technical repeats).

### Supporting Information

**Figure S1** Embryo phenotypes. A) Phenotypes of *nof1-1* embryos. Seeds were dissected after 1 hour of imbibition on whatman paper. Development ranges from globular (1) to almost fully shaped (2) embryos. B) Embryo viability using tetrazolium test (Boisson et al. 2001). Results shown are obtained with WT embryo (b) *nof1-1* embryo (c and d) and wild type embryo boiled for 30 min as negative control (a). Bar = 100 μM.

Found at: doi:10.1371/journal.pone.0012829.s001 (2.77 MB PDF)

**Figure S2** Phenotypes of *nof1-2* ovules. Siliques were dissected and cleared for DIC observations. A) row of developing ovules and B) an enlargement of the nuclei. Nuclei c–d and e exhibit typical figures of fertilized ovules whereas ovules a and b are blocked at the 4 nuclei stage of the megagametogenesis. Bar = 10 μm.

Found at: doi:10.1371/journal.pone.0012829.s002 (2.35 MB PDF)

**Figure S3** Cytological analysis of *nof1-1* embryos. A) 3D reconstructions of young embryos show defaults in cell divisions as figured onto (c) when compared to WT (a). Globular embryos show division abnormalities in the hypophysis (d,e, f) as well as in the suspensor cells, both in transverse and lengthways orientations. Bar = 10 μM B) Mature dry seeds observed using confocal scanning microscopy after modified pseudo-Schiff propidium iodide staining (a–h). Several defects are typically found in almost fully shaped *nof1-1* embryos when compared to WT (a): apical meristem is abnormal (d, arrow), ectopic divisions are found in the hypocotyl (e, f) or in the meristematic region (b) as well as defaults in cell adhesion (c). The quiescent center in the root meristem (arrow) display ectopic divisions and abnormal cellular organisation (g, WT and h, *nof1-1*). Bars = 20 μM (a, d, e, f), 15 μM (b, g, h), and 5 μM (c).

Found at: doi:10.1371/journal.pone.0012829.s003 (5.06 MB PDF)

**Figure S4** Complementation of the *nof1* mutations. The presence of the *nof1-1* or *nof1-2* T-DNA insertions was demonstrated in the progenies of transgenic seedlings by PCR using specific primers for *nof1-1* or *nof1-2* insertions (Up/RB and 2821/LB3, respectively). Kanamycin resistance of the seedlings is provided by the *nof1* mutations (see table S4) and hygromycin resistance by the new T-DNA carrying a functional copy of *NOF1* (see material and methods). Plant 6A2 is homozygous for *nof1-1*, 10B1 is homozygous for *nof1-2* and 17B3 carries both alleles. The complementation of homozygous plants for *nof1* mutations confirmed that *NOF1* mutations are responsible for the abnormal *nof1-1* and *nof1-2* phenotypes.

Found at: doi:10.1371/journal.pone.0012829.s004 (0.03 MB PDF)

**Figure S5** *NOF1* expression pattern. Electronic pictographic representations of *NOF1* expression patterns. Data analysis was performed using the tools of the Bio-Array Resource at <http://bar.utoronto.ca>. (Winter et al., 2007).

Found at: doi:10.1371/journal.pone.0012829.s005 (0.16 MB PDF)

**Figure S6** Co-expression Analyses. Functional classification of genes according to MIPS database. A) best 100 genes co-expressed with *NOF1* (input set N = 102, classified set N = 99, Atgene express tissue set) B) random list of Arabidopsis genes (input set N = 100, classified set N = 99) C) random list of Arabidopsis genes (input set N = 1000, classified set N = 976) Data analysis was performed using the tools of the Bio-Array Resource at <http://bar.utoronto.ca>. (Provart and Zhu, 2003) and the Classification superviewer software ([http://bbc.botany.utoronto.ca/ntools/cgi-bin/ntools\\_classification\\_superviewer.cgi](http://bbc.botany.utoronto.ca/ntools/cgi-bin/ntools_classification_superviewer.cgi)). Found at: doi:10.1371/journal.pone.0012829.s006 (0.06 MB PDF)

**Figure S7** Predicted network of NOF1 (At1g17690) partners. The network was build using the interaction viewer program [http://bar.utoronto.ca/interactions/cgi-bin/arabidopsis\\_interactions\\_viewer.cgi](http://bar.utoronto.ca/interactions/cgi-bin/arabidopsis_interactions_viewer.cgi). (Toufighi et al., 2005). At5g16750 Toz (TORMOZ), At2g43650 EMB2777(SAS10), At2G47990 EDA13 (SWA1 Slow Walker, UTP15), At5g66540 AtMPP10, At5g15750 AtIMP4, At4g25630 FIB2 (Fibrillarin 2), At2g41500 Emb2776 (LIS Lachesis, a WD 40 small nuclear ribonucleoprotein). Found at: doi:10.1371/journal.pone.0012829.s007 (0.21 MB PDF)

**Table S1** Segregation of the Kanamycin marker in the progenies of *nof* mutants. Cytological analyses suggesting that the mutations are embryo lethal, this hypothesis has been tested ( $H_0$  = the segregation is 2Kr/1Ks). In both cases, the observed  $X^2 > X^2$  theoretical at 5% (3,84). The data showed that the number of resistant seedlings is lower than expected for embryo lethal mutations (more especially for the null allele *nof1-2*). This suggested that the transmission of the mutated gametes was affected. Therefore, the hypothesis of a gametophytic lethal mutation has been tested for the null allele *nof1-2* (expected ratio of 1Kr/1Ks). Again the hypothesis is rejected, the observed  $X^2$  was higher than expected. The data suggested in this case that probably the two type of gametes were affected. This hypothesis was confirmed by the analyses of reciprocal crosses (see Table S2).

Found at: doi:10.1371/journal.pone.0012829.s008 (0.03 MB PDF)

**Table S2** Reciprocal crosses between hemizygous *nof1* and WT plants: occurrence of embryo lethal phenotype and segregation of the Kanamycin resistance marker. A–B–C–D: Controls. Crossing hemizygous mutants with the wild type plants, no embryo phenotypes are expected. The observed dead seeds are naturally aborted seeds usually found in wild-type siliques and/or due to manual fertilization. E–F–G–H We wished to test if the transmission of the mutated gametes is affected or not. The hypothesis  $H_0$  = the transmission is not affected or the segregation ration is 1Kr/1 Ks' was tested.  $X^2$  cut off value is 3,84 at 5% risk. For *nof1-1* (E–F), the hypothesis is accepted at 5% risk, suggesting that there was no significant effect of the transmission of *nof1-1* gametes. For the null allele, *nof1-2*, the hypothesis is clearly rejected in both cases (G and H), suggesting that both types of gametes were affected. In addition, the lack of female gamete transmission demonstrated that the mutation is female gametophytic lethal.

Found at: doi:10.1371/journal.pone.0012829.s009 (0.06 MB PDF)

**Table S3** Oligonucleotides.

Found at: doi:10.1371/journal.pone.0012829.s010 (0.02 MB PDF)

## Acknowledgments

The authors thank M. Harington for critical reading of the manuscript, V. Tanty, K. Madiona, C. Vasnier and J. Thévenin for technical supports, and M. Caboche for his constant support from the beginning of this work.

## Author Contributions

Conceived and designed the experiments: EH BD LL. Performed the experiments: EH BD JCP LL. Analyzed the data: EH BD JCP LL. Wrote the paper: EH BD LL.

## References

- Meinke DW (1995) Molecular-Genetics of Plant Embryogenesis. Annual Review of Plant Physiol and Plant Mol Biol 46: 369–394.
- Jurgens G, Mayer U, Busch M, Lukowitz W, Laux T (1995) Pattern formation in the Arabidopsis embryo: a genetic perspective. Philos Trans R Soc Lond B Biol Sci 350: 19–25.
- Meinke DW, Meinke LK, Showalter TC, Schissel AM, Mueller LA, et al. (2003) A Sequence-Based Map of Arabidopsis Genes with Mutant Phenotypes. Plant Physiol 131: 409–418.
- Lepiniec L, Devic M, Berger F (2005) Genetic and Molecular Control of Seed Development in Arabidopsis. Plant Functional Genomics. Binghamton: Food Products Press. pp 511–564.
- Shi DQ, Liu J, Xiang YH, Ye D, Sundaresan V, et al. (2005) SLOW WALKER1, essential for gametogenesis in Arabidopsis, encodes a WD40 protein involved in 18S ribosomal RNA biogenesis. Plant Cell 17: 2340–2354.
- Petricka JJ, Nelson TM (2007) Arabidopsis nucleolin affects plant development and patterning. Plant Physiol 144: 173–186.
- Griffith ME, Mayer U, Capron A, Ngo QA, Surendrarao A, et al. (2007) The TORMOZ gene encodes a nucleolar protein required for regulated division planes and embryo development in Arabidopsis. Plant Cell 19: 2246–2263.
- Fleurdepine S, Deragon JM, Devic M, Guillemont J, Bousquet-Antonelli C (2007) A bona fide La protein is required for embryogenesis in Arabidopsis thaliana. Nucleic Acids Res 35: 3306–3321.
- Jiang L, Xia M, Strittmatter LJ, Makaroff CA (2007) The Arabidopsis cohesin protein SYN3 localizes to the nucleolus and is essential for gametogenesis. Plant J 50: 1020–1034.
- Lahmy S, Guillemont J, Cheng CM, Bechtold N, Albert S, et al. (2004) DOMINO1, a member of a small plant-specific gene family, encodes a protein essential for nuclear and nucleolar functions. Plant J 39: 809–820.
- Byrne ME (2009) A role for the ribosome in development. Trends Plant Sci 14: 512–519.
- Boisvert FM, van Koningsbruggen S, Navasques J, Lamond AI (2007) The multifunctional nucleolus. Nat Rev Mol Cell Biol 8: 574–585.
- Saez Vasquez J, Medina FJ (2008) The Plant Nucleolus. Advances in Botanical Research Vol 47: 2–46.
- Brown JW, Shaw PJ (1998) Small nucleolar RNAs and pre-rRNA processing in plants. Plant Cell 10: 649–657.
- Andersen JS, Lam YW, Leung AK, Ong SE, Lyon CE, et al. (2005) Nucleolar proteome dynamics. Nature 433: 77–83.
- Pendle AF, Clark GP, Boon R, Lewandowska D, Lam YW, et al. (2005) Proteomic analysis of the Arabidopsis nucleolus suggests novel nucleolar functions. Mol Biol Cell 16: 260–269.
- Brown JWS, Shaw PJ, Shaw P, Marshall DF (2005) Arabidopsis nucleolar protein database (AtNoPDB). Nucl Acids Res 33: D633–636.
- Shaw PJ, Jordan EG (1995) The nucleolus. Annu Rev Cell Dev Biol 11: 93–121.
- Chen J, Ruan H, Ng SM, Gao C, Soo HM, et al. (2005) Loss of function of def selectively up-regulates Delta13p53 expression to arrest expansion growth of digestive organs in zebrafish. Genes Dev 19: 2900–2911.
- Baud S, Boutin JP, Miquel M, Lepiniec L, Rochat C (2002) An integrated overview of seed development in Arabidopsis thaliana ecotype WS. Plant Physiol Biochem 40: 151–160.
- Ulmasov T, Murrett J, Hagen G, Guilfoyle TJ (1997) Aux/IAA proteins repress expression of reporter genes containing natural and highly active synthetic auxin response elements. Plant Cell 9: 1963–1971.
- Geldner N, Friml J, Stierhof YD, Jurgens G, Palme K (2001) Auxin transport inhibitors block PIN1 cycling and vesicle trafficking. Nature 413: 425–428.
- Balergue S, Dubreucq B, Chauvin S, Le-Clainche I, Le Boulleire F, et al. (2001) Improved PCR-walking for large-scale isolation of plant T-DNA borders. Biotechniques 30: 496–498, 502, 504.



24. Samson F, Brunaud V, Balzergue S, Dubreucq B, Lepiniec L, et al. (2002) FLAGdb/FST: a database of mapped flanking insertion sites (FSTs) of *Arabidopsis thaliana* T-DNA transformants. *Nucleic Acids Res* 30: 94–97.
25. Libault M, Tessadori F, Germann S, Snijder B, Franz P, et al. (2005) The *Arabidopsis* LHP1 protein is a component of euchromatin. *Planta* 222: 910–925.
26. Krogan NJ, Cagney G, Yu H, Zhong G, Guo X, et al. (2006) Global landscape of protein complexes in the yeast *Saccharomyces cerevisiae*. *Nature* 440: 637–643.
27. Dunbar DA, Wormsley S, Agentis TM, Baserga SJ (1997) Mpp10p, a U3 small nucleolar ribonucleoprotein component required for pre-18S rRNA processing in yeast. *Mol Cell Biol* 17: 5803–5812.
28. Baserga SJ, Agentis TM, Wormsley S, Dunbar DA, Lee S (1997) Mpp10p, a new protein component of the U3 snoRNP required for processing of 18S rRNA precursors. *Nucleic Acids Symp Ser* pp 64–67.
29. Kamakaka RT, Rine J (1998) Sir- and silencer-independent disruption of silencing in *Saccharomyces* by Sas10p. *Genetics* 149: 903–914.
30. Bernstein KA, Gallagher JE, Mitchell BM, Granneman S, Baserga SJ (2004) The small-subunit processome is a ribosome assembly intermediate. *Eukaryot Cell* 3: 1619–1626.
31. Wehner KA, Gallagher JE, Baserga SJ (2002) Components of an interdependent unit within the SSU processome regulate and mediate its activity. *Mol Cell Biol* 22: 7258–7267.
32. Kressler D, Linder P, de La Cruz J (1999) Protein trans-acting factors involved in ribosome biogenesis in *Saccharomyces cerevisiae*. *Mol Cell Biol* 19: 7897–7912.
33. Venema J, Tollervey D (1999) Ribosome synthesis in *Saccharomyces cerevisiae*. *Annu Rev Genet* 33: 261–311.
34. Santoro R, Grummt I (2001) Molecular mechanisms mediating methylation-dependent silencing of ribosomal gene transcription. *Mol Cell* 8: 719–725.
35. Lawrence RJ, Earley K, Pontes O, Silva M, Chen ZJ, et al. (2004) A concerted DNA methylation/histone methylation switch regulates rRNA gene dosage control and nucleolar dominance. *Mol Cell* 13: 599–609.
36. Doelling JH, Pikaard CS (1995) The minimal ribosomal RNA gene promoter of *Arabidopsis thaliana* includes a critical element at the transcription initiation site. *Plant J* 8: 683–692.
37. Liang G, Klose RJ, Gardner KE, Zhang Y (2007) Yeast Jhd2p is a histone H3 Lys4 trimethyl demethylase. *Nat Struct Mol Biol* 14: 243–245.
38. Tsukada Y, Fang J, Erdjument-Bromage H, Warren ME, Borchers CH, et al. (2006) Histone demethylation by a family of JmjC domain-containing proteins. *Nature* 439: 811–816.
39. Heintzman ND, Stuart RK, Hon G, Fu Y, Ching CW, et al. (2007) Distinct and predictive chromatin signatures of transcriptional promoters and enhancers in the human genome. *Nat Genet* 39: 311–318.
40. Germann S, Juul-Jensen T, Letarnc B, Gaudin V (2006) DamID, a new tool for studying plant chromatin profiling in vivo, and its use to identify putative LHP1 target loci. *Plant J* 48: 153–163.
41. Zilberman D, Henikoff S (2007) Genome-wide analysis of DNA methylation patterns. *Development* 134: 3959–3965.
42. Weijers D, Jurgens G (2005) Auxin and embryo axis formation: the ends in sight? *Curr Opin Plant Biol* 8: 32–37.
43. Geldner N, Hamann T, Jurgens G (2000) Is there a role for auxin in early embryogenesis? *Plant Growth Regulation* 32: 187–191.
44. Hamann T, Benkova E, Baurle I, Kientz M, Jurgens G (2002) The *Arabidopsis* BODENLOS gene encodes an auxin response protein inhibiting MONOPTEROS-mediated embryo patterning. *Genes Dev* 16: 1610–1615.
45. Friml J, Vieten A, Sauer M, Weijers D, Schwarz H, et al. (2003) Efflux-dependent auxin gradients establish the apical-basal axis of *Arabidopsis*. *Nature* 426: 147–153.
46. Weijers D, Schlereth A, Ehrismann JS, Schwank G, Kientz M, et al. (2006) Auxin Triggers Transient Local Signaling for Cell Specification in *Arabidopsis* Embryogenesis. *Developmental Cell* 10: 265–270.
47. Rowland RR, Yoo D (2003) Nucleolar-cytoplasmic shuttling of PRRSV nucleocapsid protein: a simple case of molecular mimicry or the complex regulation by nuclear import, nucleolar localization and nuclear export signal sequences. *Virus Res* 95: 23–33.
48. Xue Y, Zhou F, Fu C, Xu Y, Yao X (2006) SUMOsp: a web server for sumoylation site prediction. *Nucleic Acids Res* 34: W254–257.
49. Miura K, Jin JB, Hasegawa PM (2007) Sumoylation, a post-translational regulatory process in plants. *Curr Opin Plant Biol* 10: 495–502.
50. Caperta AD, Neves N, Viegas W, Pikaard CS, Preuss S (2007) Relationships between transcription, silver staining, and chromatin organization of nucleolar organizers in *Secale cereale*. *Protoplasma* 232: 55–59.
51. Lawrence RJ, Pikaard CS (2004) Chromatin turn ons and turn offs of ribosomal RNA genes. *Cell Cycle* 3: 880–883.
52. Lewis MS, Pikaard DJ, Nasrallah M, Doelling JH, Pikaard CS (2007) Locus-specific ribosomal RNA gene silencing in nucleolar dominance. *PLoS ONE* 2: e815.
53. Chen ZJ, Pikaard CS (1997) Epigenetic silencing of RNA polymerase I transcription: a role for DNA methylation and histone modification in nucleolar dominance. *Genes Dev* 11: 2124–2136.
54. Chan SW, Henderson IR, Jacobsen SE (2005) Gardening the genome: DNA methylation in *Arabidopsis thaliana*. *Nat Rev Genet* 6: 351–360.
55. Giaever G, Chu AM, Ni L, Connelly C, Riles L, et al. (2002) Functional profiling of the *Saccharomyces cerevisiae* genome. *Nature* 418: 387–391.
56. Keener J, Dodd JA, Lalo D, Nomura M (1997) Histones H3 and H4 are components of upstream activation factor required for the high-level transcription of yeast rDNA by RNA polymerase I. *Proc Natl Acad Sci U S A* 94: 13458–13462.
57. Frescas D, Guardavaccaro D, Bassermann F, Koyama-Nasu R, Pagano M (2007) JHDM1B/FBXL10 is a nucleolar protein that represses transcription of ribosomal RNA genes. *Nature* 450: 309–313.
58. Saze H, Shiraishi A, Miura A, Kakutani T (2008) Control of genic DNA methylation by a jmjC domain-containing protein in *Arabidopsis thaliana*. *Science* 319: 462–465.
59. Braunstein M, Rose AB, Holmes SG, Allis CD, Broach JR (1993) Transcriptional silencing in yeast is associated with reduced nucleosome acetylation. *Genes Dev* 7: 592–604.
60. Dragon F, Gallagher JE, Compagnone-Post PA, Mitchell BM, Porwancher KA, et al. (2002) A large nucleolar U3 ribonucleoprotein required for 18S ribosomal RNA biogenesis. *Nature* 417: 967–970.
61. Geisler-Lee J, O'Toole N, Ammar R, Provart NJ, Millar AH, et al. (2007) A predicted interactome for *Arabidopsis*. *Plant Physiol* 145: 317–329.
62. Brady SM, Provart NJ (2009) Web-queryable large-scale data sets for hypothesis generation in plant biology. *Plant Cell* 21: 1034–1051.
63. Ruggero D, Pandolfi PP (2003) Does the ribosome translate cancer? *Nat Rev Cancer* 3: 179–192.
64. Olson MO, Dundr M, Szebeni A (2000) The nucleolus: an old factory with unexpected capabilities. *Trends Cell Biol* 10: 189–196.
65. Sirri V, Hernandez-Verdun D, Roussel P (2002) Cyclin-dependent kinases govern formation and maintenance of the nucleolus. *J Cell Biol* 156: 969–981.
66. Ptacek J, Devgan G, Michaud G, Zhu H, Zhu X, et al. (2005) Global analysis of protein phosphorylation in yeast. *Nature* 438: 679–684.
67. Dubreucq B, Berger N, Vincent E, Boisson M, Pelletier G, et al. (2000) The *Arabidopsis* AtEPR1 extensin-like gene is specifically expressed in endosperm during seed germination. *Plant J* 23: 643–652.
68. Baudry A, Caboche M, Lepiniec L (2006) TT8 controls its own expression in a feedback regulation involving TTG1 and homologous MYB and bHLH factors, allowing a strong and cell-specific accumulation of flavonoids in *Arabidopsis thaliana*. *Plant J* 46: 768–779.
69. Curtis MD, Grossniklaus U (2003) A Gateway Cloning Vector Set for High-Throughput Functional Analysis of Genes in *Planta*. *Plant Physiol* 133: 462–469.
70. Becker D (1990) Binary vectors which allow the exchange of plant selectable markers and reporter genes. *Nucleic Acids Res* 18: 203.
71. Koncz C, Kreuzaler F, Kalman Z, Schell J (1984) A simple method to transfer, integrate and study expression of foreign genes, such as chicken ovalbumin and alpha-actin in plant tumors. *Embo J* 3: 1029–1037.
72. Bechtold N, Ellis J, Pelletier G (1993) *In planta Agrobacterium* mediated gene transfer by infiltration of adult *Arabidopsis thaliana* plants. *C R Acad Sci Paris* 316: 1194–1199.
73. Chelysheva L, Diallo S, Vezon D, Gendrot G, Vrielynck N, et al. (2005) AtREC8 and AtSCC3 are essential to the monopolar orientation of the kinetochores during meiosis. *J Cell Sci* 118: 4621–4632.
74. Boisson M, Gomord V, Audran C, Berger N, Dubreucq B, et al. (2001) *Arabidopsis* glucosylase I mutants reveal a critical role of N-glycan trimming in seed development. *EMBO J* 20: 1010–1019.
75. Truernit E, Bauby H, Dubreucq B, Grandjean O, Runions J, et al. (2008) High-Resolution Whole-Mount Imaging of Three-Dimensional Tissue Organization and Gene Expression Enables the Study of Phloem Development and Structure in *Arabidopsis*. *Plant Cell*.